Exchange-correlation energy of a three-dimensional electron gas in a magnetic field

P. Skudlarski and G. Vignale
Department of Physics and Astronomy, University of Missouri–Columbia, Columbia, Missouri 65211
(Received 6 January 1993)

We present the results of random-phase-approximation calculations of the ground-state exchange and correlation energy of a uniform electron liquid in strong and intermediate magnetic fields (one or several Landau subbands populated), including arbitrary spin polarization. Applications for the current and spin-density-functional theory are discussed and appropriate effective potentials are constructed. We investigate the exchange and correlation effects on the nondissipative currents, the Landau subband occupation, and on the shape of the exchange-correlation hole. In an appendix we present a numerical fit for the exchange-correlation energy.

I. INTRODUCTION

The ground-state energy of an electron gas may be written as a sum of kinetic, exchange, and correlation terms. While the two first terms are well known, the correlation energy, being in fact the sum of all missing contributions, is available only within approximations. The calculation of the correlation energy of an electron gas is a classic problem of many-body physics. It has been developed in several steps, starting from the small and large density limits obtained by Wigner[1] and Gell-Mann and Brueckner,[2] respectively, through the random-phase approximation (RPA),[3] Hubbard,[4] and Singwi, Tosi, Land, and Sjölander (STLS) (Ref. 5) approximations, up to the stochastic, Monte Carlo calculations of Ceperley and Alder[6] which are currently considered the best available results. These approximations to the correlation energy have had many important applications, for example in the construction of the local-density approximation for the density-functional theory (thus in principle allowing most modern band-structure calculations), in determining the equilibrium properties of the electron-hole liquid,[7] and the renormalization of band gaps in doped or highly excited semiconductors.[8]

The more specialized problem of the ground-state energy of an electron gas in a magnetic field is much less developed. On the basis of the theory of the electron plasma in a magnetic field formulated by Horing and Yildiz,[9] the exchange energy was calculated by Ichimura and Tanaka[10] and later by Danz and Glasser.[11] The correlation energy is thus far known only in three limiting cases: (i) the weak magnetic-field limit in the perturbative regime ($\mu_B B \ll k_B T \ll E_F$),[12] (ii) the weak magnetic field in the de Haas–van Alphen (i.e., oscillatory) regime ($k_B T \ll \mu_B B \ll E_F$),[13] and (iii) in the superstrong magnetic-field limit ($\mu_B B \gg E_F$),[14] where all the electrons are near the bottom of the lowest Landau subband (here E_F denotes the Fermi energy, and μ is the Bohr magneton). The interest in the behavior of a three-dimensional (3D) electron gas in a magnetic field strong enough to put all the electrons in the lowest few subbands seemed to be somewhat academic to condensed-matter physicists even a few years ago, since there were no such systems experimentally available. In ordinary metals one would need magnetic fields of strength in the range of several kT to put all the electrons into the lowest Landau subband. Such fields are believed to exist only near the surface of neutron stars. Recently, however, several artificial structures have been realized in which the low density of electrons, combined with other favorable material parameters, enable us to attain the magnetic quantum limit of $l \sim a$, i.e., a magnetic length $l = \sqrt{\hbar c/eB}$, comparable to the interparticle separation a, at an accessible magnetic-field strength. For quasi-two-dimensional systems a prime example is provided by semiconductor heterostructure interfaces, where the quantum Hall effect has been observed.[15] Structures simulating a three-dimensional electron gas have also been realized recently in the form of wide parabolic quantum wells, in which the electron density can be controlled by setting the curvature of an artificially designed parabolic potential.[16] Other three-dimensional systems in which magnetic quantization can be observed include electron-hole droplets in semiconductors and large quantum dots.

In view of the development outlined above, it seems useful to present an approximate calculation of the correlation energy, not only in the limiting cases, but also in the intermediate magnetic-field regime. This is done in this paper. Our approach is based on the familiar diagrammatic many-body theory for weakly correlated systems. This is justified because the three-dimensional electron system admits a noninteracting ground state which is essentially nondegenerate. It is therefore possible to construct an approximate interacting ground state as the adiabatic continuation (at $T=0$) of the noninteracting ground state, and calculate its energy according to the standard diagrammatic procedures. This should be contrasted with the two-dimensional case, in which the massive degeneracy of the noninteracting ground state (removed here by the motion in the direction parallel to the magnetic field) forbids the application of perturbative methods.[17] Our subsequent work is based on the random-phase approximation (RPA) to the many-body theory. This approximation, in the absence of magnetic

field, is known to be asymptotically exact in the limit of large density n, that is $r_s=(3/4\pi n a_0^3)^{1/3}\ll 1$, where a_0 is the Bohr radius. With the magnetic field, this condition becomes $r_s \ll \min(1,\lambda^{2/3})$, where $\lambda \sim n l^3$ is a parameter describing the subband occupation as explained in Sec. II. In practice, even for larger values of the parameter r_s, the RPA is still a reasonable approximation of the correlation energy. More importantly, the quantity of most interest here is not the absolute value of the exchange-correlation energy, but rather its variation due to the magnetic field, i.e., $\Delta E_{\rm xc}(n,B)=E_{\rm xc}(n,B)-E_{\rm xc}(n,0)$. It is to this quantity that the RPA is applied. The absolute value of the exchange-correlation energy can then be calculated by using the value $E_{\rm xc}(n,0)$ obtained by a more accurate approximation. Previous experience[18] suggests that the RPA may be more accurate in determining energy differences, rather than the energy itself.

This paper is organized as follows. In Sec. II, we describe our system and define the basic variables and their relations. Section III presents the theoretical formulation of our calculations of the exchange-correlation energy in a magnetic field. In Sec. IV the results of the numerical calculation and the analytical limits at the subband edges are presented and discussed. Section V discusses the application of our results to the calculation of the effective potentials in the current density-functional theory (CDFT). We also calculate the coefficient of the relation between the gradient of the density and the current within local CDFT, as in Ref. 19. In Sec. VI we investigate the interacting occupation of the Landau subbands, which differs substantially from the noninteracting one. In Sec. VII we discuss the form of the exchange-correlation hole in the magnetic field with and without interaction. Finally, in the Appendix, a numerical fit for the exchange-correlation energy is given.

II. PRELIMINARY DEFINITIONS

Using the Landau gauge we can write the Hamiltonian of a 3D electron gas in a magnetic field in the second quantization picture as

$$H=\sum_{N,X,k_z,\sigma}\epsilon_{N,k_z}c^{\dagger}_{N,X,k_z,\sigma}c_{N,X,k_z,\sigma}+\frac{1}{2S}\sum_{\mathbf{q}}\sum_{N_1,X_1,k_{z1},\sigma_1,\ldots,N_4,X_4,k_{z4},\sigma_4} V(\mathbf{q})\langle N_1,X_1,k_{z1},\sigma_1|\exp(i\mathbf{q}\cdot\mathbf{r})|N_4,X_4,k_{z4},\sigma_4\rangle \times\langle N_2,X_2,k_{z2},\sigma_2|\exp(i\mathbf{q}\cdot\mathbf{r})|N_3,X_3,k_{z3},\sigma_3\rangle c^{\dagger}_{N_1,X_1,k_{z1},\sigma_1}c^{\dagger}_{N_2,X_2,k_{z2},\sigma_2} \times c_{N_3,X_3,k_{z3},\sigma_3}c_{N_4,X_4,k_{z4},\sigma_4} \quad (1)$$

Here $c_{kNX\sigma}$ and $c^{\dagger}_{kNX\sigma}$ are annihilation and creation operators for electrons described by the one-particle wave function:

$$\Psi_{kNX}(\mathbf{r})=\frac{1}{\sqrt{L_yL_z}}\exp\left[iX\frac{y}{l^2}\right]\exp(ikz)\Phi_N(x-X)\ , \quad (2)$$

$$\Phi_N(x)=\left[\frac{1}{\sqrt{\pi}l2^N N!}\right]^{1/2}H_N(x/l)\exp(-x^2/2l^2)\ , \quad (3)$$

where L_y,L_z are the sizes of the system, $l=\sqrt{\hbar c/eB}=\sqrt{\hbar/m\omega_c}$ is the magnetic length, $\Phi_N(x-X)$ is the Nth eigenfunction of a one-dimensional harmonic oscillator of cyclotron frequency $\omega_c=eB/mc$, and H_N is a Hermite polynomial. The noninteracting one-electron energy is given by

$$E(N,k_z,\sigma)=\frac{\hbar^2}{2m}k_z^2+\left[N+\tfrac{1}{2}+\sigma\frac{g}{2}\right]\hbar\omega_c\ . \quad (4)$$

The corresponding band structure is presented in Fig. 1. States defined by spin $\sigma=\pm\frac{1}{2}$, Landau subband number N, and the z component of the momentum k_z are degenerate, due to the quantization of the motion perpendicular to the magnetic field with degeneracy $G=eBS/hc$, where S is the surface of the system. Each Landau subband (characterized by N and spin σ) has its own Fermi momentum k^{σ}_{FN}. In the noninteracting case those Fermi momenta are defined by a condition of equal one-electron energy at the top of each populated subband (see Fig. 1):

$$\mu_0=\frac{\hbar^2k_{F0}^{\uparrow 2}}{2m}=\frac{\hbar^2k_{FN}^{\uparrow 2}}{2m}+N\hbar\omega_c=\frac{\hbar^2k_{FN}^{\downarrow 2}}{2m}+N\hbar\omega_c+\frac{g}{2}\hbar\omega_c\ . \quad (5)$$

Here g is the Zeeman splitting factor. It is very convenient to introduce the dimensionless variables $\bar{B}=\hbar\omega_c/\mathrm{Ry}$, and $\lambda^{\sigma}_N=k^{\sigma}_{FN}l/\sqrt{2}=k^{\sigma}_{FN}a_0/\sqrt{\bar{B}}$, where a_0

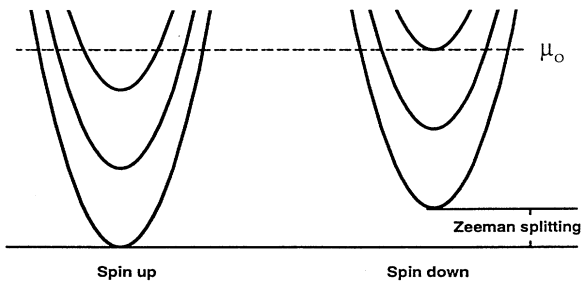

FIG. 1. The subband structure of the three-dimensional noninteracting electron gas in a magnetic field. Landau levels are replaced by parabolic Landau subbands, each filled up to its own Fermi momenta k^{σ}_{FN}.

is the Bohr radius. λ_N^σ may be interpreted as a three-dimensional filling factor for the σ-spin component of the Nth Landau subband. The density in each subband may be written similarly to the one-dimensional case, as

$$n_{\sigma N}=\frac{k_{FN}^\sigma}{\pi}\frac{G}{S}=\frac{\lambda_N^\sigma \bar{B}^{3/2}}{4\pi^2 a_0^3}\ , \tag{6}$$

The total density is proportional to the sum of all lambdas, which we will denote as $\lambda_T=\sum_{\sigma,N}\lambda_N^\sigma$ as

$$n=\frac{\lambda_T \bar{B}^{3/2}}{4\pi^2 a_0^3}\ . \tag{7}$$

The most important variable for us is the occupation factor of the lowest subband $\lambda_0^\uparrow$, which we will write for simplicity as $\lambda=\lambda_0^\uparrow$. The square of λ is proportional to the noninteracting Fermi energy $\mu_0=\lambda^2\omega_c$. This is the variable we will mostly be using to describe the occupation of the system. All the occupation factors for different subbands λ_N^σ are related to λ by relations analogous to Eq. (5):

$$\lambda_N^{\sigma 2}=\lambda^2-N-(\sigma+\tfrac{1}{2})\frac{g}{2}\ . \tag{8}$$

It is important to remember that out of three basic variables—magnetic field $\bar{B}$, density n, and occupation λ_T—any two can completely describe our system. One can easily switch between them using Eq. (7). The relation between λ and λ_T is more complicated:

$$\lambda_T=\sum_{i=0}^{N}\sqrt{\lambda^2-i}+\sum_{i=0}^{N}\left[\lambda^2-i-\frac{g}{2}\right]^{1/2}\ . \tag{9}$$

It depends on the Zeeman splitting factor g, which can vary from a very small positive number for some semiconductors to 2.0 for "ideal" electrons. One important point is to realize that at the bottom of each one-dimensional subband the density of states tends to infinity. As a result, the behavior of λ as a function of λ_T (as well as magnetic field or density) has kinks whenever the Fermi level touches a new Landau subband (for the simplest cases of $g=0$, 2, and ∞, this occurs whenever $\lambda=\sqrt{N}$ for integer N). The curves showing λ_T as a function of λ are presented in the inset of the kinetic-energy plot in Fig. 2. When we decrease the magnetic field, the number of occupied Landau subbands N and λ tends to infinity, and the distances between Landau subbands shrink to zero so that the relation between the Fermi momentum and the density changes, from strictly one dimensional $n\sim\lambda$ (for $\lambda<1.0$), to three dimensional $n\sim\lambda^2$, for large $\lambda(n\sim\lambda_T\simeq\frac{4}{3}\lambda^3\simeq\frac{4}{3}N\sqrt{N})$.

The kinetic energy per particle of the σ-spin component of the Nth subband may be written as

$$E_k(N,\sigma,\lambda,\bar{B})=\left[\frac{1}{3}\lambda^2+\left[N+\frac{1}{2}\right]+\sigma\frac{g}{2}\right]\bar{B}\ [\mathrm{Ry}]\ , \tag{10}$$

so that the total energy per particle may be written as

$$E_k(\lambda,\bar{B})=\frac{\sum_{N,\sigma}\lambda_N^\sigma E_k(N,\sigma,\lambda,\bar{B})}{\sum_{N,\sigma}\lambda_N^\sigma}\ . \tag{11}$$

In Fig. 2 we plot the curves of kinetic energy as a function of λ, at fixed density $r_s=1$. For weak magnetic field or large density, the cusps from discrete Landau subband structure fade out and we reach the well-known result $E_k=2.21/r_s^2$ Ry, valid in the absence of magnetic field.

In this paper we will assume that the Fermi momenta of subbands defined by the noninteracting Eq. (5) are not affected by interaction. In our previous paper,[20] we have shown that this is not always the case. The interaction does change the subband population, but this has no significant effect on the energy.

III. CALCULATION OF THE EXCHANGE-CORRELATION ENERGY

In order to calculate the exchange-correlation energy, we use the Hellman-Feynmann interaction strength integration technique:

$$E_{\mathrm{xc}}=\tfrac{1}{2}\int\frac{d^3q}{(2\pi)^3}V(\mathbf{q})[S_0(\mathbf{q})-1]$$
$$+\tfrac{1}{2}\int\frac{d^3q}{(2\pi)^3}V(\mathbf{q})\int_0^1 d\alpha[S_\alpha(\mathbf{q})-S_0(\mathbf{q})]\ , \tag{12}$$

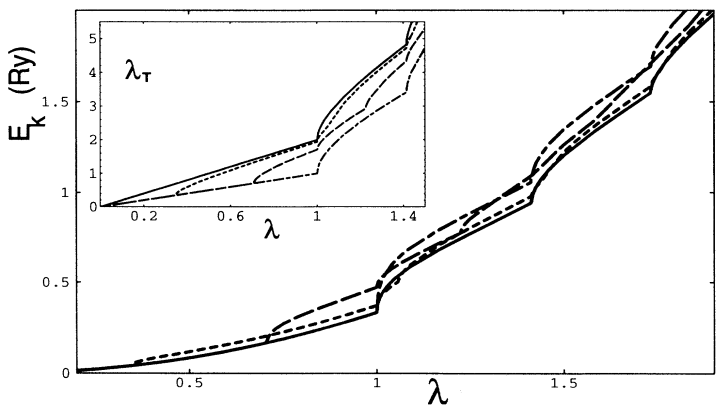

FIG. 2. The kinetic energy in Ry per particle as a function of magnetic field for fixed density at $r_s=1$. Cusps occur whenever the Fermi level crosses a new Landau subband. Curves for different values of Zeeman splitting ($g=0,0.24,1,2,\infty$) are presented *by the solid, short-dashed, long-dashed, and dashed-dotted lines, respectively.* The inset presents the total subband occupation λ_T, as a function of the lowest subband occupation λ, for those Zeeman splittings. For $\lambda\to\infty$ we have $\lambda_T\to\frac{4}{3}\lambda^3$.

where the first term is the exchange and the second is the correlation energy. Here $V(\mathbf{q})=4\pi e^2/\mathbf{q}^2$ is the Fourier transform of the Coulomb potential, $S_0(\mathbf{q})$ is the noninteracting structure factor:

$$S_0(\mathbf{q})=-\frac{1}{\pi n}\int_0^\infty d\omega\,\chi_0(\mathbf{q},i\omega)\ , \tag{13}$$

while $S_\alpha(\mathbf{q})$ is the interacting structure factor at the interaction strength α (it means substitution $e^2\rightarrow\alpha e^2$):

$$S_\alpha(\mathbf{q})=-\frac{1}{\pi n}\int_0^\infty d\omega\,\chi_\alpha(\mathbf{q},i\omega)\ . \tag{14}$$

Let us begin by evaluating the first (exchange) term. For this we have to introduce the noninteracting longitudinal polarizability

$$\chi_0(\mathbf{q},i\omega)=\sum_\sigma\int\frac{dk_z}{2\pi S}\sum_{N,M}\sum_{X,X'}\frac{f(E_{N,k_z})-f(E_{M,k_Z+q})}{i\omega+E_{N,k_z}-E_{M,k_z+q}}|\langle M,X',k_z+q_z|e^{i\mathbf{q}\cdot\mathbf{r}}|N,X,k_z\rangle|^2\ , \tag{15}$$

where $f(E_{N,k_z})$ is the Fermi-Dirac distribution function, and the matrix element of the density-fluctuation operator is given by

$$\langle M,X',k_z+q_z|e^{i\mathbf{q}\cdot\mathbf{r}}|N,X,k_z\rangle=\exp(ik_zz)\exp\left[\frac{i}{2}q_x(X'-X)\right]F_{NM}(q_\perp)\delta_{X',X+q_yl^2}\ , \tag{16}$$

where

$$F_{MN}(q_\perp)=\left[\frac{N!}{M!}\right]^{1/2}\left[\frac{(-q_y+iq_x)l}{\sqrt{2}}\right]^{M-N}\exp\left[\frac{-q_\perp^2l^2}{4}\right]L_N^{M-N}\left[\frac{q_\perp^2l^2}{2}\right] \tag{17}$$

[$L_N^\alpha(x)$ is the generalized Laguerre polynomial].

After performing the k_z integration, Eq. (15) becomes

$$\chi_0(\mathbf{q},i\omega)=\frac{-1}{4\pi^2\omega_cl^3}\sum_\sigma\sum_{N,M}\frac{|F_{MN}(q_\perp)|^2}{q_zl}\ln\left[\frac{\omega^2+\left[(N-M)\omega_c-\frac{q_z^2l^2}{2m}-\frac{k_{FN}^\sigma q_zl^2}{m}\right]^2}{\omega^2+\left[(N-M)\omega_c-\frac{q_z^2l^2}{2m}+\frac{k_{FN}^\sigma q_zl^2}{m}\right]^2}\right]\ , \tag{18}$$

here k_{FM}^σ denotes the Fermi momentum in the Mth Landau subband of spin σ. After performing the frequency and q_z integrals, we are left with a one-dimensional integral:

$$E_x(B,n)=-\frac{\sqrt{\bar{B}}}{\lambda 4\pi}\int_0^\infty dq_\perp\sum_{MM'\sigma}\left|F_{MM'}(q_\perp)\right|^2[\Psi(k_{\mathrm{FM}}^\sigma+k_{\mathrm{FM'}}^\sigma,q_\perp)-\Psi(-k_{\mathrm{FM}}^\sigma+k_{\mathrm{FM'}}^\sigma,q_\perp)+\Psi(k_{\mathrm{FM}}^\sigma-k_{\mathrm{FM'}}^\sigma,q_\perp)$$
$$+\Psi(-k_{\mathrm{FM}}^\sigma-k_{\mathrm{FM'}}^\sigma,q_\perp)]\ , \tag{19}$$

where $\Psi(x,a)=x\arctan(x/a)-(a/2)\ln(x^2+a^2)$. We have evaluated this integral numerically.

Now let us consider the correlation energy. The random-phase approximation means that we approximate the interacting polarizability as

$$\chi_\alpha(\mathbf{q},i\omega)=\frac{\chi_0(\mathbf{q},i\omega)}{1-\alpha V(\mathbf{q})\chi_0(\mathbf{q},i\omega)}\ . \tag{20}$$

After substituting it into the correlation part of Eq. (12) and performing the interaction strength integral, we obtain

$$E_c(\bar{B},\lambda)=-\frac{2\sqrt{2}\pi^2\bar{B}}{\lambda}\int_0^\infty\frac{q_\perp dq_\perp}{2\pi}\int_0^\infty\frac{dq_z}{2\pi}\int_0^\infty d\omega[Q_0(q_\perp,q_z,i\omega)-\ln|1+Q_0(q_\perp,q_z,i\omega)|]\ , \tag{21}$$

where

$$Q_0(q_\perp,q_z,i\omega)=-V(\mathbf{q})\chi_0(q_\perp,q_z,i\omega)\ . \tag{22}$$

We have performed the remaining integrals numerically.

IV. RESULTS

In Figs. 3 and 4 we present the core of our results. Here we plot the difference $\Delta E_{x,(c)}(B,n)=E_{x,(c)}(B,n)-E_{x,(c)}(0,n)$ between the exchange and the RPA correlation energies per particle calculated with magnetic field and without at fixed density $r_s=1$. The energies (in Ry) are plotted against the noninteracting chemical potential μ_0 in units of cyclotron frequency ω_c. We consider first the nonpolarized case, when both spin components have the same occupation with no Zeeman splitting (i.e., $g=0$). This method of presentation was

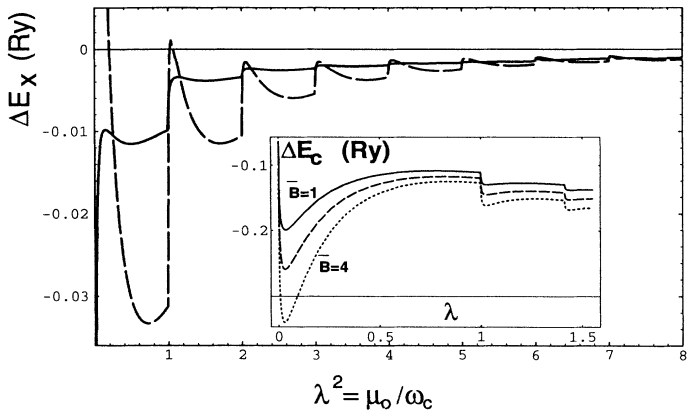

FIG. 3. The difference between the exchange energy with and without magnetic field (dashed line), calculated at constant density $r_s=1$. The solid line represents this difference for the full exchange-correlation energy. The horizontal axis represents the chemical potential in units of cyclotron frequency $\lambda^2=\mu_0/\hbar\omega_c$. In the inset the correlation energy is plotted as a function of λ at fixed magnetic field ($\bar{B}=1,2,4$). The peak of correlation energy at $\lambda\simeq 0.03$, independent of magnetic field, may be observed.

chosen for several reasons. First, we would like to make use of our calculations in reaching further than the RPA. For the electron gas without magnetic field there are several better approximations for the correlation energy (for example, Hubbard,[4] STLS,[5] Vashista-Singwi,[21] and primarily the results of the quantum Monte Carlo calculation of Ceperley and Alder[6]). We suggest that a better approximation for the correlation energy of the system in the magnetic field will be to take our data to be a measure of the strength of the magnetic-field effects, rather than using them as a final value of the energy. Our RPA results for the difference between field and no-field value should thus be added to the best available estimate of the correlation energy without magnetic field. The RPA should give a more accurate measure of the difference between these two energies, than of the correlation energy itself.[18]

Another reason for emphasizing the difference of the correlation energy with and without magnetic field is the approximate scaling property we have found. In the range of densities we are working with, $r_s=0.5-6$, we have found that for fixed $\lambda\gtrsim 0.1$ this difference scales approximately like $1/r_s$; that is,

$$\Delta E_c(\lambda,r_s)=E_c(\lambda,r_s)-E_c^{(B=0)}(r_s)$$
$$\simeq \Delta E_c(\lambda,1.0)/r_s \ . \tag{23}$$

Such a scaling property is rigorous for the exchange energy, but it does not hold for the correlation energy taken alone either with or without magnetic field. It is only the variation of the correlation energy ΔE_c that obeys Eq. (23). To demonstrate this point, in the inset of Fig. 4, we plot curves for $\Delta E_c(B,r_s)r_s$ versus B for $r_s=2$, 4, and 6. The fact that these three curves very nearly coincide demonstrates the approximate validity of Eq. (23). For a very small Fermi momentum ($\lambda\lesssim 0.1$), however, this approximate scaling relation breaks down, and should be replaced by $\Delta E_c(\lambda,r_s)\sim r_s^{-3/4}$ to provide agreement with the limiting behavior given below.

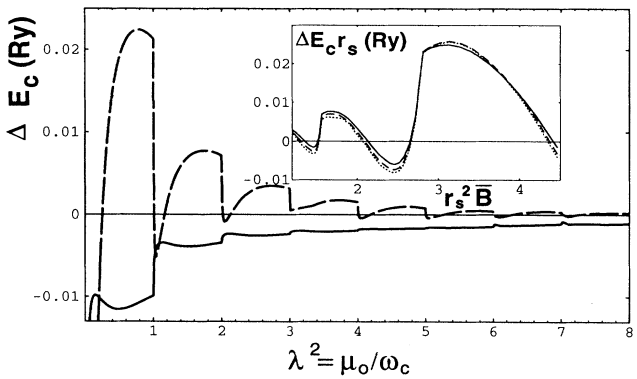

FIG. 4. The difference between the correlation energy with and without magnetic field (dashed line) calculated at constant density $r_s=1$. The solid line represents this difference for the full exchange-correlation energy. The horizontal axis represents the chemical potential in units of cyclotron frequency $\lambda^2=\mu_0/\hbar\omega_c$. The inset presents the correlation energy for three different densities multiplied by r_s, plotted vs magnetic field multiplied by r_s^2, so that the validity of the scaling property from Eq. (23) may be assessed. *The solid, dashed, and dotted lines* represents $r_s=2,4$, and 6, respectively.

The most striking feature of the data presented in Figs. 3 and 4 is that the exchange and correlation energy variations have very similar behavior although they have opposite signs and differ in overall magnitude. As a function of λ we may distinguish two regimes with different types of behavior of exchange and correlation energies.

A. Ultrastrong magnetic field ($\lambda=k_F l/\sqrt{2}\lesssim 0.3$)

In this regime the electron gas occupies only the states near the bottom of the first Landau subband, so that not only are the higher subbands empty, but even the transitions to the higher subbands may be neglected. Notice that even if the density is large, as required by the RPA, this regime is always attained in strong enough magnetic field. In this limit we have found analytically that

$$E_x(\lambda,r_s)=1.345\frac{\lambda^{2/3}}{r_s}\ln\left[\frac{\lambda}{1.679}\right] \quad (\lambda\ll 1)\ , \tag{24}$$

and, for the correlation energy

$$E_c(r_s,\lambda)=-1.606r_s^{-3/4}(1-1.009\lambda^{1/4}) \quad (\lambda\ll 1)\ , \tag{25}$$

which may also be written as

TABLE I. The RPA and Ceperley Alder (Ref. 6) results for the correlation energy of an unpolarized electron gas without magnetic field (in Ry per electron). The values of the occupation factor λ and ΔE_{xc} for two values of the magnetic-field strength ($\bar{B}=\hbar\omega_c/Ry=1,4$) are also given.

			$\bar{B}=1$		$\bar{B}=4$	
r_s	E_c^{RPA}	$E_c^{Ceperley}$	λ	ΔE_{xc}	λ	ΔE_{xc}
1	−0.157	−0.120	1.776	0.000	0.589	0.011
2	−0.124	−0.090	0.589	0.005	0.074	−0.198
3	−0.105	−0.074	0.174	−0.057	0.021	−0.237
4	−0.094	−0.064	0.074	−0.099	0.009	−0.219
5	−0.085	−0.056	0.038	−0.115	0.004	−0.195
6	−0.078	−0.051	0.021	−0.118	0.002	−0.173

$$E_c(\bar{B},\lambda)=-0.917\bar{B}^{3/8}(\lambda^{1/4}-1.009\lambda^{1/2}) \quad (\lambda\ll 1) . \tag{26}$$

In the relations for the correlation energy, only the first term was established analytically, while the second follows from a numerical fit to the results. We remind the reader that the results plotted in Figs. 3 and 4 have the zero magnetic-field values $E_x(r_s)=-0.916/r_s$ and $E_c^{RPA}(r_s)$ subtracted from them. For large density $r_s\ll 1$, the RPA correlation energy may be approximated as $E_c^{RPA}(r_s)\simeq -0.094+0.0622\ln r_s$, while at $r_s=1,\ldots,6$, the RPA correlation energy can be found in Table I.

The behavior of the correlation energy for fixed magnetic field as a function of density is also noteworthy (see Fig. 3, inset). In the small-λ regime ($nl^3\ll 1$), it varies as $n^{1/4}$, following Eq. (25). This leading contribution was established by Keldysh.[14] However, we see that it is only relevant in an extremely small range of value of $\lambda<0.04$. In this regime only the contributions of wave vectors of magnitude $|\mathbf{k}|\simeq\lambda^{1/4}\gg k_F$ and frequency $\omega\simeq\lambda^{1/2}\gg E_F$ are important to the energy integral in Eq. (12). The integral is in fact dominated by a single value of frequency, so that the density of states is not important (collective regime). For larger λ the correlation energy is controlled by the density of electron-hole excitations, which is a decreasing function of occupation number λ. As a result the correlation energy begins to decrease. This crossover from collective to electron-hole regimes is the origin of the peak observed in the inset of Fig. 3. From the form of Eq. (26) it is evident that the position of the peak is independent of magnetic field.

B. Strong and intermediate magnetic fields ($\lambda\gtrsim 0.3$)

In this regime, we observe an interesting oscillatory behavior repeating itself for each new Landau subband with decreasing amplitude. When the number of populated Landau subbands approaches eight, both the exchange and the correlation energies are within 0.2% of their values without magnetic field.

The behavior of both exchange and correlation energies at the point when a new subband begins to be populated requires a more detailed inspection. In Figs. 3 and 4 we observe strong cusps whenever population of a new Landau subband begins. Those cusps in the plot of energy against $\lambda^2=\mu_0/\omega_c$ are in fact largely enhanced by the infinite density of states on the bottom of each subband, but they would also be present if the energy were plotted against the density n, or magnetic field $\bar{B}$ (see Fig. 4, inset). For exchange energy the cusp may be easily and exactly explained. The exchange energy for a system with only a very small population λ_N of the highest Nth Landau subband may be written exactly as the sum of three terms:

$$E_x(\lambda,r_s)\sum_{i=0}^{N}\lambda_i=E_x^{(1)}(\lambda,r_s)\sum_{i=0}^{N-1}\lambda_i+E_x^{(2)}(\lambda,r_s)\lambda_N+E_x^{(3)}(\lambda,r_s)\lambda_N , \tag{27}$$

where $E_x^{(1)}$ represents the average exchange energy of the system of electrons in the lowest $N-1$ subbands; $E_x^{(2)}$ the average exchange energy of the interaction between electrons in the highest Nth subband, with all the electrons in the lower $N-1$ subbands; and $E_x^{(3)}$ the exchange per particle within the highest Nth subband only. Each of these terms can be specified as an appropriate part of the N, M sum in Eq. (15). When the Fermi level just barely passes the bottom of the Nth subband, the density of states in this subband is very large, so that nearly all new electrons are placed in it. In addition, due to the small population of the Nth subband, the $E_x^{(3)}$ contribution is very small. As a result the change in the total exchange energy is made mainly by the second term in Eq. (27). Since the exchange interaction of the electrons in the highest subband with those in the lower bands is obviously smaller than the exchange within the lower bands, the net effect is a rapid loss of exchange energy per particle, as shown by the upward cusp in Fig. 3. However, as the population of the highest subband increases, the $E_x^{(3)}$ term increases and eventually takes over, leading to the observed increase in the absolute value of the exchange energy. This increase is in fact the same as that observed in the lowest Landau subband at very small population. The expression for the correlation energy cannot be decomposed in the same way, as an exact sum of contributions from separate pairs of subbands, but in essence its cusps have the same origin. In the overall result the correlation energy largely cancels the oscillatory behavior of the exchange, but at subband edges the exchange energy cusp dominates.

The results presented up to now were obtained without including the effect of Zeeman splitting. Taking this into account now, we notice that each spin component has different Fermi momentum k_{FN}^{σ}, given by Eq. (5). Since there is no exchange interaction between electrons belonging to different spin components, the exchange energy of the system with spin populations given by $\lambda^{\uparrow}$ and $\lambda^{\downarrow}$ may be expressed easily as the sum of exchange energies for each component:

$$E_x(B,\lambda^{\downarrow},\lambda^{\uparrow})=\frac{1}{n(B,\lambda^{\downarrow})+n(B,\lambda^{\uparrow})}\times[n(B,\lambda^{\downarrow})E_x(B,\lambda^{\downarrow})+n(B,\lambda^{\uparrow})E_x(B,\lambda^{\uparrow}] , \tag{28}$$

where $n(B,\lambda)$ is the density, and $E_x(B,\lambda)$ is the exchange energy of a system with only one spin component system with a population λ, given by Eq. (19). The correlation energy cannot be found so easily because there are correlation effects between electrons with different spins. To calculate the correlation energy at a given Zeeman splitting, we have to perform the correct RPA calculation with the polarizability function χ_0 equal to the sum of polarizabilities for two spin components. We have performed those calculations for several values of g. The results (see an example in Fig. 5) show that since new Landau subbands in each spin component begin to be populated at different values of λ, each cusp connected with a new Landau subband is split into two, one for each spin component. Additionally a new peak occurs at a very strong magnetic field ($\lambda=\sqrt{g}/2$) when the down-spin component begins to be populated (this peak cannot be seen at Fig. 5). One has to take into account that, due to the interaction driven shift in the subband occupation, the position of the cusps may change significantly, as described in our previous work.[20]

Remarkably, we find that the result of the exact calculation is very well approximated by an average of the correlation energy for the unpolarized electron gas at densities $\lambda^{\uparrow}$ and $\lambda^{\downarrow}$, i.e.,

$$\Delta E_c(B,\lambda^{\downarrow},\lambda^{\uparrow}) \simeq \frac{1}{n(\lambda^{\downarrow})+n(\lambda^{\uparrow})}[n(\lambda^{\downarrow})\Delta E_c(B,\lambda^{\downarrow}) + n(\lambda^{\uparrow})\Delta E_c(B,\lambda^{\uparrow})] , \tag{29}$$

Here $\Delta E_c(B,\lambda)$ denotes the difference between the correlation energy of a state with both spin components equally filled, and occupation factor λ and the correlation energy of a state of the same density calculated without magnetic field. Figure 5 presents the result of the exact RPA calculations (solid line), and that of the approximate formula of Eq. (29) for $g=0.24$ (dashed line). The difference between the two curves is clearly very small, so Eq. (29) may be used to construct the numerical fit (see Appendix).

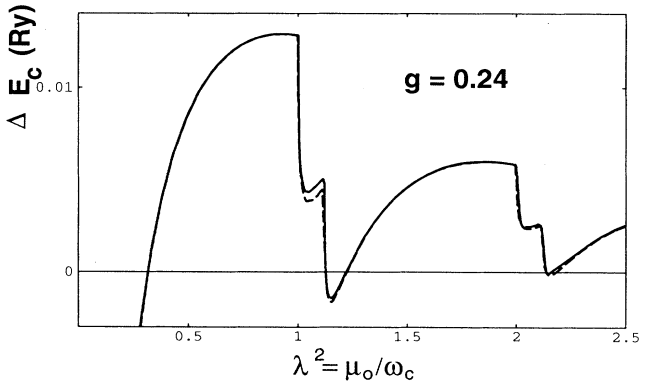

FIG. 5. The difference between the correlation energy with and without magnetic field for the polarized electron gas at the physical value of the Zeeman splitting ($g=0.24$), and at fixed density ($r_s=2$). The solid line represents the results of full RPA calculations, while the dashed line was approximated using Eq. (29). The accuracy of the approximation may be assessed.

V. APPLICATIONS TO THE CURRENT-DENSITY-FUNCTIONAL THEORY

We present here some applications of our results to the current-density-functional theory (CDFT). The CDFT (Ref. 23) is a generalization of the density-functional theory (DFT) (Refs. 24 and 25) which includes the coupling of orbital currents to the magnetic field. The central object in density-functional theories is an energy functional of some intensive variables. For example, in the spin-density-Functional Theory (SDFT) (Refs. 26 and 27) the magnetic field is included, but only insofar as it couples to the electron spins one writes

$$\mathcal{E}_{xc}[n^{\uparrow}(\mathbf{r}),n^{\downarrow}(\mathbf{r})]=\int n(\mathbf{r})E_{xc}(n^{\uparrow}(\mathbf{r}),n^{\downarrow}(\mathbf{r})) , \tag{30}$$

where $E_{xc}(n^{\uparrow}(\mathbf{r}),n^{\downarrow}(\mathbf{r}))$ is the exchange-correlation energy per particle of a uniform system with arbitrary spin densities $n^{\uparrow}(\mathbf{r}),n^{\downarrow}(\mathbf{r})$. In CDFT the basic intensive variables are the spin densities $n^{\uparrow}(\mathbf{r}),n^{\downarrow}(\mathbf{r})$ and the paramagnetic current density $\mathbf{j}_p(\mathbf{r})$. However, the exchange-correlation part of the energy functional depends on $\mathbf{j}_p$ only via the vorticity $\nu=\nabla\times\mathbf{j}_p/n$. Therefore the functional $\mathcal{E}_{xc}$ does not allow the local approximation in the terms of currents, but one can construct a local approximation in terms of the vorticity $\nu=\nabla\times(\mathbf{j}_p/n)$. It has been shown that a state of uniform spin density and vorticity can be identified as a state of uniform spin density in a uniform magnetic field $\mathbf{B}=-mc|\nu|/e$.[23] Thus we obtain

$$\mathcal{E}_{xc}[n^{\uparrow}(\mathbf{r}),n^{\downarrow}(\mathbf{r}),\nu(\mathbf{r})] = \int n(\mathbf{r})E_{xc}[n^{\uparrow}(\mathbf{r}),n^{\downarrow}(\mathbf{r}),\mathbf{B}=-mc|\nu(\mathbf{r})|/e] , \tag{31}$$

We see that the local approximation for $\mathcal{E}_{xc}$ is completely determined by the knowledge of the energy of a uniform system $E_{xc}(n^{\uparrow}(\mathbf{r}),n^{\downarrow}(\mathbf{r}),B)$, which we have calculated in the previous section.

The determination of the ground-state density and current in CDFT can be achieved by solving the Kohn-Sham equations:

$$\left[\frac{1}{2m}\left[-i\hbar\nabla+\frac{e}{c}\mathbf{A}_{eff}(\mathbf{r})\right]^2+V_{eff}(\mathbf{r})\right]\Psi_i(\mathbf{r})=\epsilon_i\Psi_i(\mathbf{r}) . \tag{32}$$

Here the effective potentials $\mathbf{A}_{eff}(\mathbf{r})$ and $V_{eff}(\mathbf{r})$ are given by

$$\mathbf{A}_{eff}(\mathbf{r})=\mathbf{A}(\mathbf{r})+\mathbf{A}_{xc}(\mathbf{r}) , \tag{33}$$

$$V_{eff}(\mathbf{r})=V(\mathbf{r})+V_H(\mathbf{r})+V_{xc}(\mathbf{r})+\frac{e^2}{2mc^2}[\mathbf{A}^2-\mathbf{A}_{eff}^2] , \tag{34}$$

and the number density and paramagnetic current density are defined in terms of Kohn-Sham orbitals as

$$n(\mathbf{r})=\sum_i |\Psi_i(\mathbf{r})|^2 ,$$
$$\mathbf{j}_p(\mathbf{r})=-\frac{i\hbar}{2m}\sum_i \{\Psi_i^*(\mathbf{r})\nabla\Psi_i(\mathbf{r})-[\nabla\Psi_i^*(\mathbf{r})]\Psi_i(\mathbf{r})\} . \quad (35)$$

The *exchange-correlation part* of effective potentials are functionals of the spin density and current distributions given by

$$V_{\rm xc}^{\sigma}(\mathbf{r})=\left.\frac{\delta\mathcal{E}_{\rm xc}[n^{\uparrow}(\mathbf{r}),n^{\downarrow}(\mathbf{r}),v(\mathbf{r})]}{\delta n^{\sigma}(\mathbf{r})}\right|_{v} , \quad (36)$$

$$\mathbf{A}_{\rm xc}(\mathbf{r})=\frac{1}{n(\mathbf{r})}\nabla\times\left.\frac{\delta\mathcal{E}_{\rm xc}[n^{\uparrow}(\mathbf{r}),n^{\downarrow}(\mathbf{r}),v(\mathbf{r})]}{\delta\mathbf{j}_p(\mathbf{r})}\right|_{n} . \quad (37)$$

In the local-density approximation (LDA) the $\mathcal{E}_{\rm xc}[n^{\uparrow}(\mathbf{r}),n^{\downarrow}(\mathbf{r}),v]$ functional is approximated by Eq. (31), and we can explicitly carry out the derivatives in Eqs. (36) and (37). This gives

$$V_{\rm xc}^{\sigma}(\mathbf{r})=\frac{\partial[n(\mathbf{r})E_{\rm xc}(n^{\uparrow}(\mathbf{r}),n^{\downarrow}(\mathbf{r}),B(\mathbf{r}))]}{\partial n^{\sigma}(\mathbf{r})} \quad (38)$$

$$\mathbf{A}_{\rm xc}(\mathbf{r})=-\frac{mc}{ne}\left[\frac{\partial^2 E_{\rm xc}(n^{\uparrow}(\mathbf{r}),n^{\downarrow}(\mathbf{r}),B(\mathbf{r}))}{\partial B\,\partial n}(\nabla n)\times\hat{B}+\frac{\partial^2 E_{\rm sc}(n^{\uparrow}(\mathbf{r}),n^{\downarrow}(\mathbf{r}),B(\mathbf{r}))}{\partial B^2}\nabla\times\mathbf{B}(\mathbf{r})\right] , \quad (39)$$

where

$$\mathbf{B}(\mathbf{r})=-\frac{mc}{e}\nabla\times\frac{\mathbf{j}_p}{n}$$
$$=\mathbf{B}_0(\mathbf{r})-\nabla\times\frac{\mathbf{j}}{n}\left[\frac{mc}{e}\right]-\int\frac{\mathbf{j}(\mathbf{r}')\times(\mathbf{r}-\mathbf{r}')}{|\mathbf{r}-\mathbf{r}'|^3}d\mathbf{r}' . \quad (40)$$

Here we have assumed for simplicity that the direction of the vorticity versor $\hat{v}$ is approximately constant and parallel to the $\hat{z}$ direction. In Fig. 6 we present the scalar exchange-correlation potential $V_{\rm xc}(\mathbf{r})$ as a function of density for several strengths of magnetic field ($\bar{B}=1,2,4$). We notice that for large density the effects of magnetic field are weak, and curves for different $\bar{B}$ nearly coincide with the curve obtained without magnetic field. However, when the density decreases we approach the quantum regime ($\lambda<1$) and the curves starts to deviate (strong magnetic field first, weaker later). If we look at our results at fixed magnetic field (see inset), we can see that the magnetic-field dependence of the potential has oscillations and discontinuities at Landau subband edges, but those changes are much weaker than the density dependence (compare the scale of the main plot and inset). Those results were obtained for a system with no Zeeman splitting ($g=0$), when $V_{\rm xc}^{\uparrow}=V_{\rm xc}^{\downarrow}$. For an arbitrary value of Zeeman splitting, the $V_{\rm xc}^{\uparrow}$ and $V_{\rm xc}^{\downarrow}$ will be different, yet the difference is very small, and occurs only near the subband edges. For example, for $g=0.24$ this difference would be invisible in the scale of our plot.

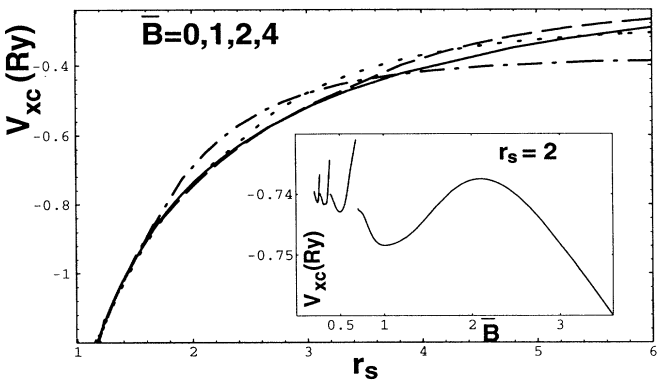

FIG. 6. The effective scalar exchange-correlation potential as a function of density at fixed magnetic field. The solid line presents results obtained without magnetic field. Dashed, dotted, and dotted-dashed lines were calculated at magnetic field strength of $\bar{B}=$ 1, 2, and 4, respectively. We notice that at high density all the curves coincide. When the density decreases, the effect of magnetic field is visible, first for strong, then for weaker magnetic fields. The inset presents the magnetic-field dependence of the effective potential plotted at fixed density ($r_s=2$). Oscillations and discontinuities connected with Landau subbands can be noticed. The absolute value of the magnetic-field effects is much smaller than that of the density: compare the scales of the inset and the main figure.

A problem arises when we try to apply our results for densities near to subband edges. The potentials are discontinuous there. Taking into account the repopulation of subbands discussed in Ref. 20 will shift the positions and significantly decrease the size of discontinuities, but will not cancel it. Physically those discontinuities reflect the sudden appearance of new types of orbitals when the Fermi level crosses the bottom of a new Landau subband. The effect is similar to the discontinuity of the exchange-correlation potential in semiconductors, except that in our case the LDA is already sufficient to describe it qualitatively.

As we have mentioned before, the CDFT may be used to determine the currents in the nonuniform system as in Ref. 28. In the uniform system, due to translational symmetry currents must vanish everywhere, but if the density is nonuniform the system in the magnetic field will spontaneously develop nonvanishing currents. In our previous paper[19] we derived the following local CDFT relation between the gradient of the density and current:

$$\mathbf{j}(\mathbf{r})=\frac{\hbar}{2m}\gamma[n(\mathbf{r}),B_0(\mathbf{r})]\nabla n(\mathbf{r})\times\hat{z}\ , \tag{41}$$

where

$$\gamma=\frac{2mc}{e}\left[1+n\frac{\partial}{\partial n}\right]\frac{\partial E}{\partial B_0}[n(\mathbf{r}),B_0(\mathbf{r})]\ . \tag{42}$$

For a very strong magnetic-field ($\lambda\to 0$) limit, the kinetic energy dominates, which leads to $\gamma=1$. Our formula for the currents then reduces to the formula obtained by Girvin and MacDonald[29] on the assumption that the one-electron wave functions belong completely to the first Landau subband. The derivatives of the energy functional $\mathcal{E}_{\rm xc}$ may be performed using the results from Sec. IV, while the kinetic part of gamma γ_k may be derived easily from our discussion of Fermi momentum in Sec. II. It may be written as

$$\gamma_k=1-2\frac{\sum_{n,\sigma}k_{FN\sigma}l-N(k_{FN\sigma}l)^{-1}}{\sum_{n,\sigma}(k_{FN\sigma}l)^{-1}}\ . \tag{43}$$

The results for γ_k are presented in Fig. 7 (upper panel) against chemical potential $\lambda=k_F l/\sqrt{2}$. Not surprisingly, they show sharp discontinuities whenever a new Landau subband is being populated, and so they depend strongly on the Zeeman splitting factor g which defines the relative positions of Landau subbands in both spin components. Here we plot by a solid line the result with no Zeeman splitting $g=0$ (identical to the case with infinite one $g=\infty$). For a physical value of $0<g\ll 2$ each discontinuity is split into two, one for each spin component which begins to be occupied at a given λ.

In the lower panel of Fig. 7 we present the contribution of exchange-correlation effects to γ for different densities (one has to notice that while the kinetic contribution depends on the density only via the dimensionless Fermi momentum λ, the exchange-correlation distribution is strongly density dependent). The smaller the density the larger the exchange-correlation contribution. In the range of densities of our interest ($0.5<r_s<6$) we can see that the exchange-correlation corrections are much smaller than the kinetic part. In the strong magnetic-field limit $\lambda\to 0$ both the exchange and correlation correction tends to 0, while at the subband edges $\lambda^2\to 1,2,\ldots$, they have logarithmic singularities, which cancel each other giving in effect finite discontinuities in the exchange-correlation contribution. For most practical applications we may disregard the exchange and correlation contributions to the γ factor.

VI. INTERACTING OCCUPATION OF LANDAU SUBBANDS

The simple noninteracting picture of Landau subbands filled uniformly up to the Fermi momentum is changed seriously by the electron-electron interaction. The wave functions characterized by the Landau subband number and the momentum parallel to the magnetic field are no longer eigenfunctions of the full Hamiltonian. The interaction mixes states belonging to different subbands, and as a result changes their occupations. The occupations of Landau subbands may be expressed as the expectation value of an operator:

$$\hat{N}_{L\sigma}=\sum_{k_z,X}\hat{c}^{+}_{Lk_zX\sigma}\hat{c}_{Lk_zX\sigma}\ , \tag{44}$$

where $\hat{c}^{+}_{Lk_zX\sigma}$, $\hat{c}_{Lk_zX\sigma}$ are defined in Sec. II. In terms of the Green's function it is given by

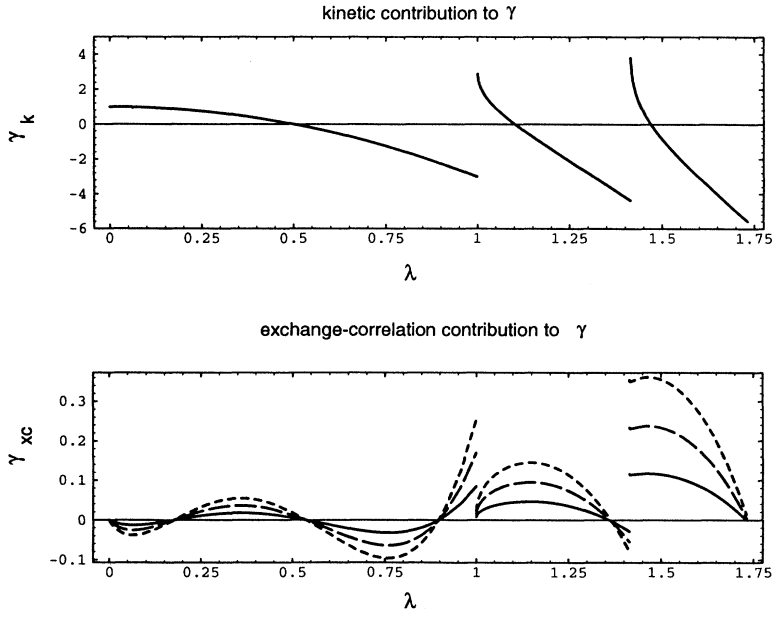

FIG. 7. Upper panel: kinetic contribution to $\gamma(n,B_0)$, Eq. (42), as a function of noninteracting Fermi momentum $\lambda=k_F l/\sqrt{2}$. Solid line represents results for both spinless ($g=\infty$) and nonpolarized ($g=0$) electrons. Lower panel: exchange-correlation contribution to $\gamma(n,B_0)$, for spinless electrons ($g=\infty$). The solid, dashed, and dotted lines present results obtained for the density $r_s=1,2,3$, respectively.

$$n_{L\sigma}=\frac{\langle \hat{N}_{L\sigma}\rangle}{V}=\lim_{\eta\to 0}\frac{1}{2\pi l^2}\int\frac{d\omega}{2\pi}\int\frac{d^3k}{2\pi}G_{L\sigma}(k,i\omega)e^{i\omega\eta}\ . \tag{45}$$

Here we have included only the diagonal in terms of the Green's function $G_{LL\sigma\sigma}(\mathbf{k},i\omega)=G_{L\sigma}(\mathbf{k},i\omega)$, and self-energy $\Sigma_{LL\sigma\sigma}(\mathbf{k},i\omega)=\Sigma_{L\sigma}(\mathbf{k},i\omega)$ in the spin and Landau subband representation. This can be done because in the uniform system all off-diagonal terms vanish. To see this let us write the full expansion of the Green's function as

$$G(\mathbf{r},\mathbf{r}';i\omega)=\sum_{N,N'}\sum_{X,X'}\sum_{k_z,k_z'}G_{N,X,N',X'}(k_z,k_z';i\omega)\Psi_{NXk_z}(\mathbf{r})\Psi^*_{N'X'k_z'}(\mathbf{r}')\ . \tag{46}$$

In the Landau gauge, the invariance under the translation in the y direction imposes $X'=X$, and the invariance under the magnetic translation in the x direction makes $G_{N,X,N',X}(\mathbf{k},\mathbf{k}';i\omega)$ independent of X. Finally the rotational invariance can be satisfied only if $N=N'$.

After some standard manipulation,[30] we can express the change in the Lth subband occupation number due to the electron-electron interactions as

$$\delta n_{L\sigma}=n_{L\sigma}-n^{(0)}_{L\sigma}=\lim_{\eta\to 0}\frac{1}{2\pi l^2}\mathrm{Im}\int\frac{d\omega}{2\pi}\int\frac{d^3k}{2\pi}\left[-\frac{\partial}{\partial\omega}\ln\frac{G_{L\sigma}(\mathbf{k},i\omega)}{G^{(0)}_{L\sigma}(\mathbf{k},i\omega)}+G_{L\sigma}(\mathbf{k},i\omega)\frac{\partial\Sigma_{L\sigma}(\mathbf{k},i\omega)}{\partial\omega}\right]e^{i\omega_n\eta}\ . \tag{47}$$

The frequency integral of the first term works out to be equal to the complex phase of the Green's function at $\omega=0$, which vanishes because of the exact property $\mathrm{Im}\Sigma_{L\sigma}(k,0)=0$. Thus we are left with

$$\delta n_{L\sigma}=-\frac{1}{2\pi l^2}\mathrm{Im}\int\frac{d\omega}{2\pi}\int\frac{d^3k}{2\pi}\Sigma_{L,\sigma}(\mathbf{k},i\omega)\frac{\partial}{\partial\omega}G_{L\sigma}(\mathbf{k},i\omega)\ . \tag{48}$$

In the RPA the self-energy is written as

$$\Sigma_{L\sigma}(\mathbf{k},i\omega)=\int\frac{d^3q}{(2\pi)^3}\int\frac{d\omega}{2\pi}\int\frac{d\Omega}{2\pi}V(\mathbf{q})\frac{Q_0(\mathbf{q},i\Omega)}{1+Q_0(\mathbf{q},i\Omega)}\sum_M|F_{LM}(q_\perp)|^2G^{(0)}_{M\sigma}(\mathbf{k}+\mathbf{q},i\omega+i\Omega)\ , \tag{49}$$

where $Q_0(\mathbf{q},i\omega)$ is defined in Eq. (22). The integrals in Eq. (48) may be carried out numerically. It is important to point out that if we used the Hartree-Fock approximation the occupation shift would be zero. This can be easily seen from Eq. (47) and the fact that $\Sigma^{\mathrm{HF}}(\mathbf{k})$ is independent of frequency. Thus the effect we are discussing here appears only when we include the correlation effects.

In Fig. 8 we present our results. Here by solid lines we plot the noninteracting occupations of the lowest Landau subbands as a function of λ. The dashed lines represent the interacting occupations calculated using Eq. (48). We notice that even when the noninteracting picture predicts that only a small fraction of the lowest subband is occupied, we have noticeable occupation of higher subbands. A similar phenomenon is known to occur for systems without magnetic field. One finds there that, even at $T=0$, there is a long tail of states with $k>k_F$, which have a finite occupation. Notice that the total occupation of each spin component (summed over all subbands) remains unaffected by the interaction. This is consistent with the fact that electron-electron-scattering processes may change the subband population, but cannot change the total spin of interacting particles.

It is important to keep in mind that we assume here that the ground state of the interacting Hamiltonian may be obtained by adiabatically switching on the interaction from the *ground state* of the noninteracting Hamiltonian. The change of the subband occupation, which we have discussed above, is a reflection of the fact that the interacting Hamiltonian is mixing the eigenstates of the noninteracting one. Yet this is only one mechanism in which the interaction is affecting the subband occupation. The other one is based on the following observation. The assumption that the interacting ground state can be obtained in the process of adiabatic continuation from the noninteracting ground state is *incorrect*. In our recent paper[20] we proved that to obtain the interacting state of the lowest energy we must perform an adiabatic continuation of a noninteracting state which is different from the noninteracting ground state. The above procedure of cal-

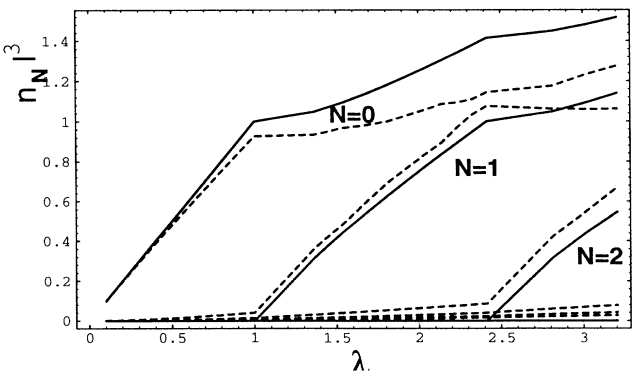

FIG. 8. The interacting occupation of Landau subbands (dashed line) compared to the noninteracting one (solid line). One can notice that the interaction creates a finite population of higher subbands even if in the noninteracting case they would be completely empty.

culating the subband occupation was applied there using the noninteracting polarizability $\chi_0(\mathbf{q},i\omega)$ defined in Eq. (18) with Fermi momenta k_{FN}^{σ} adjusted to minimize the total interacting ground-state energy.

VII. EXCHANGE-CORRELATION HOLE

The exchange-correlation hole is given by $h(\mathbf{r}_\perp,\mathbf{r}_z)=n[g(\mathbf{r}_\perp,\mathbf{r}_z)-1]$, where $g(\mathbf{r}_\perp,\mathbf{r}_z)$ is the pair distribution function which is given by the Fourier transform of the structure factor:

$$S(\mathbf{q}_\perp,q_z)=-\frac{1}{\pi n}\int_0^\infty d\omega\,\chi(\mathbf{q}_\perp,q_z,i\omega)\ . \tag{50}$$

The RPA calculation for $\chi(\mathbf{q},i\omega)$ has been discussed in Sec. III. Let us first consider the exchange hole, which is obtained by substituting $\chi=\chi_0$ in Eq. (50). If we express lengths in units of magnetic length l, then the shape of the distribution function depends only on λ (i.e., it does not depend on the strength of the magnetic field and density separately). In the limit of weak magnetic field ($\lambda\to\infty$) the exchange hole is isotropic, and its size is given by $r_\perp=r_z\simeq n^{-1/3}\simeq l\lambda_T^{-1/3}$. On the other hand, in the limit of the strong magnetic field ($\lambda<1$) the size of the hole is $r_\perp\simeq l$, $r_z\simeq l/\lambda\gg l$. In the intermediate regime we have: $r_\perp\simeq l(\lambda/\lambda_T)^{1/2}$, $r_z\simeq l/\lambda$. So except for small kinks at the subband edges, the eccentricity of the exchange hole increases monotonically with increasing magnetic field, but the effect is important only for the strong magnetic field (e.g., at $\lambda=1 r_z/r_\perp\simeq 1.3$).

Since the interaction is isotropic, we would expect that it will pull the hole toward a more symmetric shape, and this is what actually happens. In Fig. 9 we present the shape of exchange and exchange-correlation holes for different magnetic fields ($\lambda=0.1$, 0.5, and 1.5) and different densities ($r_s=1,4$). Here we plot the equidensity lines at which $g(\mathbf{r}_\perp,r_z)=0.5$. We notice that while the noninteracting exchange hole (solid line) is strongly elongated at $\lambda=0.1$ and 0.5, the interaction reduces the eccentricity. The interaction effect is weaker for $r_s=1$ (dotted line) than for the more dilute system at $r_s=4$ (dashed line). This elongation of the exchange-correlation hole occurs only for very strong magnetic field; at $\lambda=1.5$, when the third Landau subband is populated, even the exchange hole is nearly isotropic.

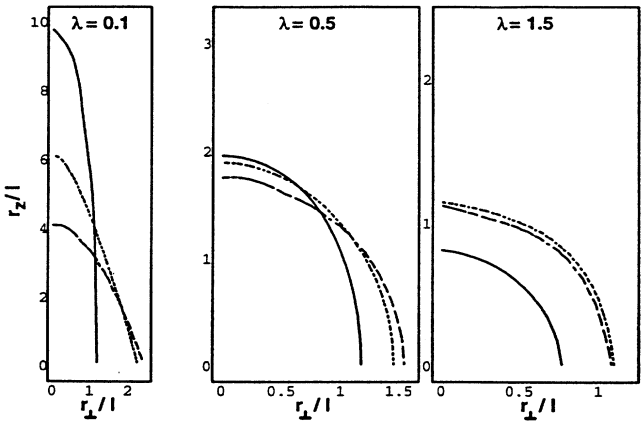

FIG. 9. The shape of the exchange-correlation hole. The lines of equal value of the distribution function $g(r_\perp,r_z)=0.5$ are plotted. The solid line represents the exchange hole. The dotted line shows the exchange-correlation hole at large density $r_s=1$, which means relatively weak interaction. The dashed line was obtained at $r_s=4$. We can see that at very small λ (strong magnetic field) the exchange hole is elongated in the magnetic-field direction, yet the interaction pulls it back to a more spherical shape. This anisotropy can only be seen for very strong magnetic fields. When the third Landau subband is being populated ($\lambda=1.5$), even the exchange hole is nearly isotropic.

ACKNOWLEDGMENTS

We thank Professor A. H. MacDonald for several useful discussions. We acknowledge many important contributions from our recently deceased friend and collaborator Dr. Mark Rasolt. This work was supported in part by the National Science Foundation Grant No. DMR-9100988 and by the Donors of the Petroleum Research Fund administered by the American Chemical Society.

APPENDIX. NUMERICAL FIT FOR THE EXCHANGE-CORRELATION ENERGY

Here we present the fit for the exchange-correlation energy of the unpolarized ($g=0$) electron gas as a function of λ, at a density of $r_s=1$. The results for different densities within a range $0.5<r_s<6.0$ may be obtained by using the scaling relation of Eq. (23). It is important to remember that this approximate scaling relation is not correct for very small $\lambda<0.1$. Thus our fit does not describe the density dependence in the ultrastrong magnetic-field regime, but it is satisfactory in most of the physically interesting region. To get the result for the spin-polarized gas, one has to use Eqs. (28) and (29).

As discussed in Sec. IV, we fit the difference between the actual energy and the energy obtained at the same density without magnetic field $\Delta E_{\rm xc}=E_{xc}-E_{xc}^{(B=0)}$. Let us define $y=\lambda^2-[\lambda^2]$, where $[\lambda^2]$ denotes the integer part of λ^2. Depending on the number of Landau levels occupied, we may write the exchange-correlation energy in Ry per electron as follows.

For $\lambda<1$,

$$\Delta E_{\rm xc}(\lambda)=1.128\,33\lambda^{0.25}-0.975\,816\lambda+0.533\,489\lambda^2 -0.163\,083\lambda^3+0.117\,75\lambda^{2/3}\ln(\lambda)-0.532\ . \tag{A1}$$

For $1<\lambda<\sqrt{2}$,

$$\Delta E_{\rm xc}=0.0022(y^2-y)-0.0023\ . \tag{A2}$$

For $\sqrt{2}\le\sqrt{N}<\lambda<\sqrt{N+1}$ (here $N+1$ is an integer—number of occupied Landau subbands),

$$\Delta E_{\rm xc}=0.000\,26N+0.003(y^2-y)/N-0.002\ . \tag{A3}$$

For strong magnetic field ($\lambda<1$) the agreement between the fit and results of the full calculation is very good. For higher Landau subbands ($N>2$) the cancellation of exchange and correlation is very strong, so that our numerical results cannot give the precise shape of the subband

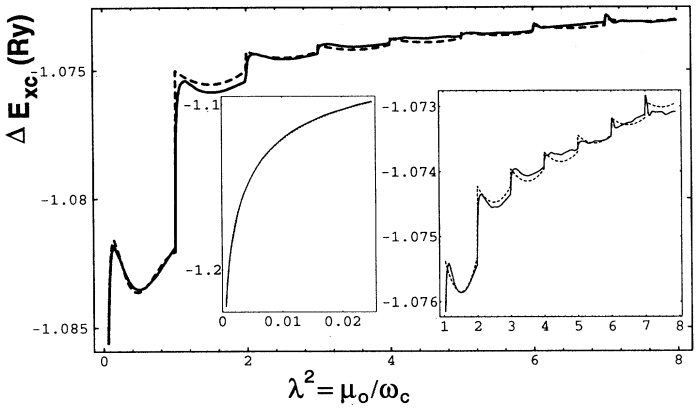

FIG. 10. The accuracy of the fit given in the Appendix may be assessed by a comparison between the calculated value of the exchange-correlation energy (with the zero-field energy subtracted) represented by the solid line, and its numerical fit given in the Appendix and represented by the dashed line. The insets present enlargements of the superstrong and weak magnetic-field regions.

edges. Therefore only the average value and general curvature of the function between subband edges is represented in the fit. The accuracy of this fit may be assessed from Fig. 10. To obtain the full exchange-correlation energy our results for ΔE_{xc} should be added to the exchange-correlation energy without magnetic field. In Table I we provide the RPA (see, e.g., Ref. 22) and Ceperley-Alder[6] values of correlation energy without magnetic field, and our magnetic-field correction for two different values of the magnetic field.

The Ceperley-Alder results may be approximated by the Perdew-Zunger formula, as given in Ref. 31.

For $r_s \geq 1$,

$$E_c(r_s) = -0.2846/(1+1.0529\sqrt{r_s}+0.3334 r_s) . \quad \text{(A4)}$$

For $r_s \leq 1$,

$$E_c(r_s) = 0.0622 \ln r_s - 0.096 + 0.004 r_s \ln r_s - 0.0232 r_s . \quad \text{(A5)}$$

Summarizing, to calculate the exchange-correlation energy of an electron gas in the magnetic field of strength B and density of spin components $n^{\uparrow}, n^{\downarrow}$, one has to do the following:

(1) Calculate $\lambda_T^{\uparrow}$ and $\lambda_T^{\downarrow}$ using formula (7): $n^{\uparrow,\downarrow} = \lambda_T^{\uparrow,\downarrow} \bar{B}^{3/2}/4\pi^2 a_0^3$.

(2) Calculate the dimensional Fermi momentum $\lambda^{\uparrow,\downarrow}$ for each spin component using relation (9): $\lambda_T^{\uparrow,\downarrow} = \sum_{i=0}^{N} \sqrt{(\lambda^{\uparrow,\downarrow})^2 - i}$, where N is the integer part of $(\lambda^{\uparrow,\downarrow})^2$.

(3) Using the numerical fit presented in this appendix in Eqs. (A1)–(A3), calculate $\Delta E_{xc}^{\uparrow,\downarrow}(\lambda^{\uparrow,\downarrow}, r_s = 1)$.

(4) Using the scaling relation for density Eq. (23), calculate

$$\Delta E_{xc}^{\uparrow,\downarrow}(\lambda^{\uparrow,\downarrow}, r_s^{\uparrow,\downarrow}) = \Delta E_x c^{\uparrow,\downarrow}(\lambda^{\uparrow,\downarrow}, r_s = 1)/r_s^{\uparrow,\downarrow} .$$

(5) Using Eqs. (28) and (29) calulate $\Delta E_{xc}(B, n^{\uparrow}, n^{\downarrow}) = \Delta E_{xc}(\lambda^{\uparrow}, \lambda^{\downarrow}, r_s)$ as

$$\Delta E_{xc}(\lambda^{\downarrow}, \lambda^{\uparrow}, r_s) = \frac{1}{n(\lambda^{\downarrow}) + n(\lambda^{\uparrow})} [n(\lambda^{\downarrow}) \Delta E_{xc}(\lambda^{\downarrow}, r_s^{\downarrow}) + n(\lambda^{\uparrow}) \Delta E_{xc}(\lambda^{\uparrow}, r_s^{\downarrow})] .$$

(6) Calculate the exchange-correlation energy of an electron gas of given density and spin polarization without magnetic field, using the best available approximation. For nonpolarized case one can use the Pardew-Zunger formula given above in Eqs. (A4) and (A5) (see also Ref. 31).

(7) Add the magnetic-field correction from step (5) to the no-field result from step (6) to obtain the total exchange-correlation energy in the magnetic field.

[1]E. P. Wigner, Phys. Rev. **2**, 1002 (1934).
[2]M. Gell-Mann and K. A. Brueckner, Phys. Rev. **106**, 364 (1957).
[3]See, e.g., P. Nozières, *Theory of Interacting Fermi Systems* (Benjamin, New York, 1964).
[4]J. Hubbard, Proc. R. Soc. London Ser. A **243**, 336 (1957).
[5]K. S. Singwi, M. P. Tosi, R. H. Land, and A. Sjölander, Phys. Rev. **176**, 589 (1968).
[6]D. M. Ceperley and B. J. Alder, Phys. Rev. Lett. **45**, 566 (1980).
[7]T. M. Rice, in *Solid State Physics,* edited by H. Ehrenreich, F. Seitz, and D. Turnbull (Academic, New York, 1977), Vol. 32, p. 1.
[8]G. Tränkle, H. Leier, A. Forchel, H. Haug, C. Ell, and G. Weimann, Phys. Rev. Lett. **58**, 419 (1987); M. Capizzi, S. Modesti, A. Frova, J. L. Staehli, M. Guzzi, and R. A. Logan, Phys. Rev. B **29**, 2028 (1984).
[9]N. J. Horing, Ann. Phys. (N.Y.) **31**, 1 (1965); N. J. M. Horing, M. Orman, and M. Yildiz, Phys. Lett. **48A**, 7 (1974); N. J. M. Horing and M. Yildiz, Ann. Phys. (N.Y.) **97**, 216 (1976).
[10]H. Ichimura and S. Tanaka, Prog. Theor. Phys. **25**, 315 (1961).
[11]R. W. Danz and M. L. Glasser, Phys. Rev. B **4**, 94 (1971); M. L. Glasser and J. I. Kaplan, Ann. Phys. (N.Y.) **73**, 1 (1972).
[12]G. Vignale, M. Rasolt, and D. J. W. Geldart, Phys. Rev. B **37**, 2502 (1988).
[13]J. M. Luttinger, Phys. Rev. B **5**, 1251 (1961).
[14]L. V. Keldysh and T. A. Onishchenko, Pis'ma Zh. Eksp. Teor. Fiz. **24**, 70 (1976) [JETP Lett. **24**, 59 (1976)]; L. V. Keldysh, in *Proceedings of the International School of Physics "Enrico Fermi," Course 89* (North-Holland, Amsterdam 1985), pp. 644–683.
[15]See, e.g., *Quantum Hall Effect,* edited by Richard E. Prange

and Steven M. Girvin (Springer-Verlag, New York 1987).
[16]E. G. Gwinn, R. M. Vestervelt, P. F. Hopkins, A. J. Rimberg, M. Sundaram, A. J. Rimberg, and R. M. Westervelt, Phys. Rev. B **40**, 3970 (1989); M. Shayegan, T. Sajoto, M. Santos, and C. Silvestre, Appl. Phys. Lett. **53**, 791 (1988).
[17]R. B. Laughlin, Phys. Rev. Lett. **50**, 1395 (1983); D. Yoshioka and P. A. Lee, Phys. Rev. B **27**, 4986 (1988).
[18]Most of the error in the RPA calculations comes from the contribution of the region of large momentum transfer **q** to the exchange-correlation integral of Eq. (12). In this region, the polarizability calculated with magnetic field tends asymptotically to its no-field value. In effect, this overestimation [resulting in the nonphysical negative value of the pair distribution function $g(\mathbf{r})$ for small **r**] is similar in both cases, and largely cancels when we calculate the difference of field and no-field value of the correlation energy.
[19]G. Vignale and P. Skudlarski, Phys. Rev. B **46**, 10 232 (1992).
[20]P. Skudlarski and G. Vignale, Phys. Rev. Lett. **69**, 949 (1992).
[21]Vashista and K. S. Singwi, Phys. Rev. B **6**, 875 (1972).
[22]K. S. Singwi and M. P. Tosi, in *Solid State Physics,* edited by H. Ehrenreich, F. Seitz, and D. Turnbull (Academic, New York, 1977), Vol. 36, p. 177.
[23]G. Vignale and M. Rasolt, Phys. Rev. Lett. **59**, 2360 (1987); Phys. Rev. B **37**, 10 685 (1988); M. Rasolt and G. Vignale, Phys. Rev. Lett. **65**, 1498 (1990); G. Vignale, M. Rasolt, and D. J. W. Geldart, Adv. Quantum Chem. **21**, 235 (1990).
[24]P. Hohenberg and W. Kohn, Phys. Rev. **136**, B864 (1964).
[25]W. Kohn and L. J. Sham, Phys. Rev. **140**, A1133 (1965).
[26]U. von Barth and L. Hedin, J. Phys. C **5**, 1629 (1972).
[27]O. Gunnarsson and B. I. Lundqvist, Phys. Rev. B **13**, 4274 (1976).
[28]P. Skudlarski, G. Vignale, and M. Rasolt, Phys. Rev. B **45**, 8494 (1992).
[29]A. H. MacDonald and S. M. Girvin, Phys. Rev. B **38**, 6295 (1988).
[30]See, e.g., A. A. Abrikosov, L. P. Gorkov, and I. E. Dzyaloshinski, *Methods of Quantum of Field Theory in Statistical Physics* (Dover, New York, 1975), Chap. III.
[31]J. P. Perdew and Alex Zunger, Phys. Rev. B **23**, 5048 (1981). For a wider discussion of different parametrizations of the correlation energy of an electron gas without magnetic field, see also J. M. MacLaren, D. P. Clougherty, M. E. McHenry, and M. M. Donovan, Comp. Phys. Commun. **66**, 383 (1991).